MOX-Report No. 14/2019

Mixed-primal Discontinuous Galerkin approximation of flows in fractured porous media on polygonal and polyhedral grids

Antonietti, P.F.; Facciolà, C; Verani, M.

MOX, Dipartimento di Matematica
Politecnico di Milano, Via Bonardi 9 - 20133 Milano (Italy)

mox-dmat@polimi.it http://mox.polimi.it

Mixed-primal Discontinuous Galerkin approximation of flows in fractured porous media on polygonal and polyhedral grids *

Paola F. Antonietti[#], Chiara Facciolà[#] and Marco Verani[#]

May 27, 2019

[#] MOX- Laboratory for Modeling and Scientific Computing
Dipartimento di Matematica
Politecnico di Milano
Piazza Leonardo da Vinci 32, 20133 Milano, Italy

paola.antonietti@polimi.it, chiara.facciola@polimi.it, marco.verani@polimi.it

Abstract

We propose a formulation based on discontinuous Galerkin methods on polygonal/polyhedral grids for the simulation of flows in fractured porous media. We adopt a model for single-phase flows where the fracture is modelled as a $(d-1)$ - dimensional interface in a d - dimensional bulk domain and the flow is governed by the Darcy's law in both the bulk and the fracture. The two problems are then coupled through physically consistent conditions. We focus on the numerical approximation of the coupled bulk-fracture problem, discretizing the bulk problem in mixed form and the fracture problem in primal form. We present an priori h- and p-version error estimate in a suitable (mesh-dependent) energy norm and numerical tests assessing it.

1 Introduction

The problem of modelling the flow in a fractured porous medium is fundamental in many energy or environmental engineering applications such as tracing oil migration, isolation of radioactive waste, groundwater contamination, etc. Many Geophysical and Engineering applications, are characterized by a strong complexity of the physical domain, possibly involving thousands of fault/fractures, heterogeneous media, and complex topographies. For example, a fractured oil reservoir can be cut by several thousands of fractures, which often intersect, create small angles or are nearly coincident. For this reason, in realistic cases, the construction of a computational grid aligned with the fractures is still a major issue. Indeed, whenever classical Finite-Element-based approaches are employed to discretize the underlying differential model, the process of mesh generation can be the bottleneck of the whole simulation, as classical finite elements only support computational grids composed

*Paola F. Antonietti and Chiara Facciolà have been partially supported by SIR Starting grant n. RBSI14VT0S "PolyPDEs: Non-conforming polyhedral finite element methods for the approximation of partial differential equations" funded by MIUR. All the authors have been partially supported by INdAM-GNCS.

by tetrahedral/hexahedral/prismatic elements. To overcome this limitation, in the last decade a wide strand of literature focused on the design of numerical methods that support computational meshes composed of general polygonal and polyhedral (polytopic, for short) elements. Within this framework, we focus our attention on developing a numerical approximation of the coupled bulk-fracture model based on polytopic Discountinuous Galerkin (PolyDG) methods. In particular, the intrinsic "discontinuous" nature of DG methods allows very general polytopic elements because of the freedom in representing the underlying (local) polynomial space. Indeed the degrees of freedom are not "attached" to any geometric quantity (vertexes, edges, etcc), so that mesh elements with edges/faces that may be in arbitrary number and whose measure may be arbitrarily small compared to the diameter of the corresponding element are naturally supported with a solid theoretical background. This approach is then very well suited to tame the geometrical complexity featured by most of applications in the computational geoscience field. Moreover, since the interface conditions between the bulk and fracture problem can be naturally formulated using jump and average operators, the coupling of the two problems can be naturally embedded in the variational formulation. In particular, we discretize the problem in the bulk in mixed form employing the local DG (LDG) method of [5] and the problem in the fracture in primal form using the Symmetric Interior Penalty discontinuous Galerkin method [9, 2], both in their generalization to polytopic grids. This is an extension of the work [1], where a primal-primal discretization is considered.

2 Mathematical model

For simplicity, we consider the case of a porous medium cut by a single, non immersed fracture. The porous matrix is represented by the domain $\Omega \subset \mathbb{R}^d$, $d = 2, 3$, which we assume to be open, bounded, convex and polygonal/polyhedral. Following the strategy of [6], we suppose that the fracture may be described by the $(d-1)$-dimensional $\mathcal{C}^\infty$ manifold (with no curvature) $\Gamma \subset \mathbb{R}^{d-1}$, $d = 2, 3$. This approach is justified by the fact that the thickness of the fracture domain is typically some orders of magnitude smaller than the size of the domain. The fracture separates Ω into two connected disjoint subdomains, $\Omega \setminus \Gamma = \Omega_1 \cup \Omega_2$ with $\Omega_1 \cap \Omega_2 = \emptyset$. We decompose the boundary of Ω into two disjoint subsets $\partial\Omega_D$ and $\partial\Omega_N$, *i.e.*, $\partial\Omega = \partial\Omega_D \cup \partial\Omega_N$, with $\partial\Omega_D \cap \partial\Omega_N = \emptyset$. Moreover, $\partial\Gamma = \Gamma \cap \partial\Omega$, $\partial\Gamma = \partial\Gamma_D \cup \partial\Gamma_N$. Finally, we denote by $\mathbf{n}_i$, $i = 1, 2$ the unit normal vector to Γ pointing outwards from Ω_i and, for a (regular enough) scalar-valued function q and a (regular enough) vector-valued function $\mathbf{v}$, we define the classical *jump* and *average* operators across the fracture Γ as

$$\begin{aligned} \{q\} &= \frac{1}{2}(q_1 + q_2) \qquad & [\![q]\!] &= q_1\mathbf{n}_1 + q_2\mathbf{n}_2, \\ \{\mathbf{v}\} &= \frac{1}{2}(\mathbf{v}_1 + \mathbf{v}_2) \qquad & [\![\mathbf{v}]\!] &= \mathbf{v}_1 \cdot \mathbf{n}_1 + \mathbf{v}_2 \cdot \mathbf{n}_2, \end{aligned} \tag{1}$$

where the subscript $i = 1, 2$ denotes the restriction to the subdomain Ω_i.

We now introduce the governing equations for the model. We suppose that the flow is governed by Darcy's law both in the bulk and along the fracture, where we formulate a reduced version of the law in the tangential direction. We formulate the problem in the bulk in mixed form and the problem in the fracture in primal form. The model is then closed by interface conditions that couple the two problems along their interface. Given

the source terms $f \in L^2(\Omega)$ and $f_\Gamma \in L^2(\Gamma)$ and the boundary data $g_D \in H^{1/2}(\partial\Omega_D)$ and $g_\Gamma \in H^{1/2}(\partial\Gamma)$, the coupled bulk-fracture model reads as follows:

$$\begin{cases} \mathbf{u}_i = \boldsymbol{\nu}_i \nabla p_i & \text{in } \Omega_i, \\ -\nabla \cdot \mathbf{u}_i = f_i & \text{in } \Omega_i, \\ p = g_D & \text{on } \partial\Omega_D, \\ \mathbf{u} \cdot \mathbf{n} = 0 & \text{on } \partial\Omega_N, \\ -\nabla_\tau \cdot (\boldsymbol{\nu}_\Gamma^\tau \ell_\Gamma \nabla_\tau p_\Gamma) = f_\Gamma - [\![\mathbf{u}]\!] & \text{in } \Gamma, \\ p_\Gamma = g_\Gamma & \text{on } \partial\Gamma_D, \\ (\boldsymbol{\nu}_\Gamma^\tau \nabla_\tau p_\Gamma) \cdot \boldsymbol{\tau} = 0 & \text{on } \partial\Gamma_N, \\ -\{\mathbf{u}\} = \beta_\Gamma [\![p]\!] & \text{on } \Gamma, \\ -[\![\mathbf{u}]\!] = \alpha_\Gamma (\{p\} - p_\Gamma) & \text{on } \Gamma. \end{cases} \tag{2}$$

In the bulk equations, $\boldsymbol{\nu} = \boldsymbol{\nu}(x) \in \mathbb{R}^{d\times d}$ is the bulk permeability tensor, which we assume to be symmetric, positive definite, uniformly bounded from below and above and with entries that are bounded, piecewise continuous real-valued functions. In the fracture equations, $\ell_\Gamma > 0$ denotes the fracture thickness, $\boldsymbol{\tau}$ is the vector in the tangent plane of Γ normal to $\partial\Gamma$ and the symbols ∇_τ and $\nabla_\tau\cdot$ denote the tangential gradient and divergence operators, respectively. Moreover, we assume that the fracture permeability tensor $\boldsymbol{\nu}_\Gamma$, has a block-diagonal structure of the form $\boldsymbol{\nu}_\Gamma = \begin{bmatrix} \nu_\Gamma^n & 0 \\ 0 & \boldsymbol{\nu}_\Gamma^\tau \end{bmatrix}$, when written in its normal and tangential components and that $\boldsymbol{\nu}_\Gamma^\tau \in \mathbb{R}^{(d-1)\times(d-1)}$ is a positive definite, uniformly bounded tensor (it reduces to a positive number for $d = 2$). We also assume that $\boldsymbol{\nu}_\Gamma$ satisfies the same regularity assumptions as those satisfied by the bulk permeability $\boldsymbol{\nu}$. In the coupling conditions, the constants β_Γ and α_Γ are defined as $\beta_\Gamma = \frac{1}{2\eta_\Gamma}$ and $\alpha_\Gamma = \frac{2}{\eta_\Gamma(2\xi-1)}$, with $\eta_\Gamma = \frac{\ell_\Gamma}{\nu_\Gamma^n}$. In the definition of α_Γ, the closure parameter $\xi > 1/2$ is related to the pressure profile across the fracture aperture. We refer to [6] for a rigorous derivation of the model.

3 Numerical formulation based on PolyDG methods

We now introduce the DG-discretization of problem (2), based on the Local Discontinuous Galerkin method (LDG) [5] for the bulk problem and on the Symmetric Interior Penalty method (SIPDG) [2, 9] for the fracture problem, both in their generalization to polytopic grids [4]. The LDG method is a particular DG method that can be included in the class of mixed finite element methods. However, the variable $\mathbf{u}_h$ can be *locally* solved in terms of p_h and then eliminated from the equations, giving rise to a primal formulation where p_h is the only unknown. In what follows, we present the formulation of the bulk problem in a mixed setting. However, we remark that, it is possible to recast in a primal setting, in order to perform the analysis in the framework of [3, 7].

For the problem in the bulk, we consider a family of meshes $\mathcal{T}_h$ made of disjoint open *polygonal/polyhedral* elements. No limitation on either the number of faces of each polygon $E \in \mathcal{T}_h$ or on the relative size of the faces compared to the diameter of the element is imposed. We consider meshes $\mathcal{T}_h$ that are aligned with the fracture Γ, so that any element $E \in \mathcal{T}_h$ cannot be cut by Γ and it belongs exactly to one of the two disjoint subdomains Ω_1 or Ω_2. This implies that each mesh $\mathcal{T}_h$ induces a subdivision of the fracture Γ into faces, which we denote by Γ_h. It follows that, if we define the set $\mathcal{F}_h$ of all the faces of

the elements in $\mathcal{T}_h$, we can write $\mathcal{F}_h = \mathcal{F}_h^I \cup \mathcal{F}_h^B \cup \Gamma_h$, where $\mathcal{F}_h^B$ is the set of faces lying on the boundary of the domain $\partial\Omega$ and $\mathcal{F}_h^I$ is the set of interior faces not belonging to the fracture. In addition, we write $\mathcal{F}_h^B = \mathcal{F}_h^D \cup \mathcal{F}_h^N$, where $\mathcal{F}_h^D$ and $\mathcal{F}_h^N$ are the boundary faces contained in $\partial\Omega_D$ and $\partial\Omega_N$, respectively (we assume the decomposition to be matching with the partition of $\partial\Omega$ into $\partial\Omega_D$ and $\partial\Omega_N$). We denote by $\mathcal{E}_{\Gamma,h}$ the set of all the edges of the elements in Γ_h, and we write, accordingly to the previous notation, $\mathcal{E}_{\Gamma,h} = \mathcal{E}_{\Gamma,h}^I \cup \mathcal{E}_{\Gamma,h}^B$, with $\mathcal{E}_{\Gamma,h}^B = \mathcal{E}_{\Gamma,h}^D \cup \mathcal{E}_{\Gamma,h}^N$. For each element $E \in \mathcal{T}_h$, we denote by $|E|$ its measure, by h_E its diameter and we set $h = \max_{E\in\mathcal{T}_h} h_E$. Given an element $E \in \mathcal{T}_h$, for any face $F \subset \partial E$, with $F \in \mathcal{F}_h$, we define $\mathbf{n}_F$ as the unit normal vector on F that points outward of E. Analogous definitions may be also set up on the fracture. Finally, on a face F, we can then define for (regular enough) scalar and vector-valued functions v and $\boldsymbol{\tau}$ the standard jump and average operators similarly to (1), if $F \in \mathcal{F}_h \setminus \mathcal{F}_h^B$ and as $[\![q]\!] = q\mathbf{n}_F$ and $\{\mathbf{v}\} = \mathbf{v}$, if $F \in \mathcal{F}_h^B$.

Regarding the functional setting, we will employ the following notation. For an open, bounded domain $D \subset \mathbb{R}^d$, $d = 2, 3$, we will denote by $H^s(D)$ the standard Sobolev space of order s, for a real number $s \geq 0$. Given a decomposition of the domain into elements $\mathcal{T}_h$, we will denote by $H^s(\mathcal{T}_h)$ the standard *broken* Sobolev space, equipped with the broken norm $||\cdot||_{s,\mathcal{T}_h}$. Furthermore, we will denote by $\mathbb{P}_k(D)$ the space of polynomials of *total* degree less than or equal to $k \geq 1$ on D. The symbol $\lesssim$ (and $\gtrsim$) will signify that the inequalities hold up to multiplicative constants which are independent of the discretization parameters, but might depend on the physical parameters.

For simplicity, we will suppose that the permeability tensors $\boldsymbol{\nu}$ and $\boldsymbol{\nu}_\Gamma$ are piecewise *constant* on mesh elements. Moreover, we set $\bar{\boldsymbol{\nu}}_E = |\sqrt{\boldsymbol{\nu}|_E}|_2^2$ and $\bar{\boldsymbol{\nu}}_F^\tau = |\sqrt{\ell_\Gamma \boldsymbol{\nu}_\Gamma^\tau|_F}|_2^2$, where $|\cdot|_2$ denotes the l_2-norm.

The DG discrete problem will be set in the following spaces:

$$
\begin{aligned}
Q_h^b &= \{q \in L^2(\Omega) : \ q|_E \in \mathbb{P}_{k_E}(E) \ \forall E \in \mathcal{T}_h\},\\
\mathbf{W}_h^b &= \{\mathbf{v} \in [L^2(\Omega)]^d : \ \mathbf{v}|_E \in [\mathbb{P}_{k_E}(E)]^d \ \forall E \in \mathcal{T}_h\},\\
Q_h^\Gamma &= \{q_\Gamma \in L^2(\Gamma) : \ q_\Gamma|_F \in \mathbb{P}_{k_F}(F) \ \forall F \in \Gamma_h\}.
\end{aligned}
$$

The DG discretization of the bulk-fracture problem (2) reads ad follows:
Find $\big((p_h, \mathbf{u}_h), p_h^\Gamma\big) \in Q_h^b \times \mathbf{W}_h^b \times Q_h^\Gamma$ such that

$$
\begin{aligned}
\mathcal{M}_b(\mathbf{u}_h, \mathbf{v}) + \mathcal{B}_b(p_h, \mathbf{v}) &= F_b(\mathbf{v}) && \forall \mathbf{v} \in \mathbf{W}_h^b,\\
-\mathcal{B}_b(q, \mathbf{u}_h) + \mathcal{S}_b(p_h, q) + \mathcal{I}_1(p_h, q, p_{\Gamma,h}) &= G_b(q) && \forall q \in Q_h^b,\\
\mathcal{A}_\Gamma(p_{\Gamma,h}, q_\Gamma) + \mathcal{I}_2(p_h, p_{\Gamma,h}, q_\Gamma) &= \mathcal{L}_\Gamma(q_\Gamma) && \forall q_\Gamma \in Q_h^\Gamma,
\end{aligned}
\tag{3}
$$

where the bilinear forms are defined as

$$\begin{aligned}
\mathcal{M}_b(\mathbf{u}_h,\mathbf{v}) &= \int_{\mathcal{T}_h} \boldsymbol{\nu}^{-1}\mathbf{u}_h\cdot\mathbf{v},\\
\mathcal{B}_b(p_h,\mathbf{v}) &= -\int_{\mathcal{T}_h}\nabla p_h\cdot\mathbf{v}+\int_{\mathcal{F}_h^I}[\![p_h]\!]\cdot(\{\mathbf{v}\}-\mathbf{b}[\![\mathbf{v}]\!])+\int_{\mathcal{F}_h^D}p_h\mathbf{v}\cdot\mathbf{n}_F,\\
\mathcal{S}_b(p_h,q) &= \int_{\mathcal{F}_h^I\cup\mathcal{F}_h^D}\sigma_F[\![p_h]\!]\cdot[\![q]\!],\\
\mathcal{I}_1(p_h,q,p_{\Gamma,h}) &= \int_{\Gamma_h}\beta_\Gamma[\![p_h]\!]\cdot[\![q]\!]+\int_{\Gamma_h}\alpha_\Gamma(\{p_h\}-p_{\Gamma,h})\{q\},\\
F_b(\mathbf{v}) &= \int_{\mathcal{F}_h^D} g_D\mathbf{v}\cdot\mathbf{n}_F,\\
G_b(q) &= \int_{\mathcal{T}_h} fq+\int_{\mathcal{F}_h^D}\sigma_F g_D q,\\
\mathcal{A}_\Gamma(p_{\Gamma,h},q_\Gamma) &= \int_{\Gamma_h}\boldsymbol{\nu}_\Gamma^\tau\ell_\Gamma\nabla_\tau p_\Gamma\cdot\nabla_\tau q_\Gamma+\int_{\mathcal{E}_{\Gamma,h}^I\cup\mathcal{E}_{\Gamma,h}^D}\big(-\{\boldsymbol{\nu}_\Gamma^\tau\ell_\Gamma\nabla_\tau p_{\Gamma,h}\}\cdot[\![q_\Gamma]\!]-\{\boldsymbol{\nu}_\Gamma^\tau\ell_\Gamma\nabla_\tau q_\Gamma\}\cdot[\![p_{\Gamma,h}]\!]\\
&\quad+\int_{\mathcal{E}_{\Gamma,h}^I\cup\mathcal{E}_{\Gamma,h}^D}\sigma_e^\Gamma[\![p_{\Gamma,h}]\!]\cdot[\![q_\Gamma]\!]\big),\\
\mathcal{I}_2(p_h,p_{\Gamma,h},q_\Gamma) &= \int_{\Gamma_h}\alpha_\Gamma(p_{\Gamma,h}-\{p_h\})q_\Gamma,\\
\mathcal{L}_\Gamma(q_\Gamma) &= \int_{\Gamma_h} f_\Gamma q_\Gamma-\int_{\mathcal{E}_{\Gamma,h}^D}(\boldsymbol{\nu}_\Gamma^\tau\ell_\Gamma\nabla_\tau q_\Gamma\cdot\boldsymbol{\tau}-\sigma_e^\Gamma q_\Gamma)g_\Gamma.
\end{aligned}$$

Here, we have introduced the vector-valued function $\mathbf{b}\in[L^\infty(\mathcal{F}_h^I)]^d$, which is constant on each face, and the bulk penalty function $\sigma:\mathcal{F}_h\setminus\Gamma_h\to\mathbb{R}^+$, defined facewise as

$$\sigma(\mathbf{x})=\sigma_0\begin{cases}\max_{E\in\{E^+,E^-\}}\frac{\bar{\boldsymbol{\nu}}_E k_E^2}{h_E} & \text{if } \mathbf{x}\subset F\in\mathcal{F}_h^I,\ \bar{F}=\partial\bar{E}^+\cap\partial\bar{E}^-,\\ \frac{\bar{\boldsymbol{\nu}}_E k_E^2}{h_E} & \text{if } \mathbf{x}\subset F\in\mathcal{F}_h^D,\ \bar{F}=\partial\bar{E}\cap\partial\bar{\Omega},\end{cases}\tag{4}$$

with $\sigma_0>0$ independent of k_E, $|E|$ and $|F|$. The fracture penalty function $\sigma^\Gamma:\mathcal{E}_{\Gamma,h}\to\mathbb{R}^+$ is defined analogously.

4 Well-posedness and error estimates

We introduce the following *energy* norm on the discrete space $Q_h^b\times Q_h^\Gamma$

$$\begin{aligned}
|||(q,q_\Gamma)|||^2 = ||\boldsymbol{\nu}^{1/2}\nabla q||_{0,\mathcal{T}_h}^2+||\sigma_F^{1/2}[\![q]\!]||_{0,\mathcal{F}_h^I\cup\mathcal{F}_h^D}^2+||(\boldsymbol{\nu}_\Gamma^\tau\ell_\Gamma)^{1/2}\nabla q_\Gamma||_{0,\Gamma_h}^2+||\sigma_e^{1/2}[\![q_\Gamma]\!]||_{0,\mathcal{E}_{\Gamma,h}^I\cup\mathcal{E}_{\Gamma,h}^D}^2\\
+||\beta_\Gamma^{1/2}[\![q]\!]||_{0,\Gamma_h}^2+||\alpha_\Gamma^{1/2}(\{q\}-q_\Gamma)||_{0,\Gamma_h}^2
\end{aligned}\tag{5}$$

Definition 4.1. A mesh $\mathcal{T}_h$ is said to be *polytopic-regular* if, for any $E\in\mathcal{T}_h$, there exists a set of non-overlapping (not necessarily shape-regular) d-dimensional simplices $\{S_E^i\}_{i=1}^{n_E}$ contained in E, such that $\bar{F}=\partial\bar{E}\cap\bar{S_E^i}$, for any face $F\subseteq\partial E$, and $h_E\lesssim\frac{d|S_E^i|}{|F|}$, $i=1,\dots,n_E$,

with the hidden constant independent of the discretization parameters, the number of faces of the element n_E, and the face measure.

We remark that this definition does not give any restriction on the number of faces per element, nor on their measure relative to the diameter of the element the face belongs to. If we assume that $\mathcal{T}_h$ and Γ_h are polytopic-regular meshes, we can state the following well-posedness result, which is a direct consequence of Lax-Milgram's Lemma.

Proposition 4.1. *Let the penalization parameters σ for the problem in the bulk and in the fracture be defined as in* (4)*. Then, the fully-coupled discrete problem* (3) *is well-posed provided that $\sigma_{0,\Gamma}$ is chosen big enough.*

Next, we state an a-priori error estimate for the discrete problem (3). All the theory behind the error analysis of PolyDG-methods is based on the extension of standard *hp*-approximation bounds on simplices to arbitrary polytopic elements [4]. To do so, some technical assumptions and definitions are required. Here we summarize the fundamental ones. For each subdomain Ω_i, $i = 1, 2$, we denote by $\mathscr{E}_i$ the classical continuous extension operator $\mathscr{E}_i : H^s(\Omega_i) \to H^s(\mathbb{R}^d)$, for $s \in \mathbb{N}_0$. Similarly, we denote by $\mathscr{E}_\Gamma$ the continuous extension operator $\mathscr{E}_\Gamma : H^s(\Gamma) \to H^s(\mathbb{R}^{d-1})$, for $s \in \mathbb{N}_0$. We then make the following regularity assumptions for the exact solution $(p, \mathbf{u}, p_\Gamma)$ of problem (2):

Assumption 4.2. *Let $\mathcal{T}_\# = \{T_E\}$ be a covering of Ω related to the polytopic mesh $\mathcal{T}_h$, i.e. a set of shape-regular d-dimensional simplices T_E, such that for each $E \in \mathcal{T}_h$, there exists a $T_E \in \mathcal{T}_\#$ such that $E \subsetneq T_E$. We assume that the exact solution p is such that $p \in H^2(\mathcal{T}_h)$ and $[\![\boldsymbol{\nu}\nabla p]\!] = 0$ on $\mathcal{F}_h^I$. Moreover, for every $E \in \mathcal{T}_h$, if $E \subset \Omega_i$, it holds $\mathscr{E}_i p_i|_{T_E} \in H^{r_E}(T_E)$, with $r_E \geq 1 + d/2$ and $T_E \in \mathcal{T}_\#$ with $E \subset T_E$. Similarly, let $\mathcal{F}_\# = \{T_F\}$ be a simplex covering of Γ. We assume that the exact solution p_Γ is such that $p_\Gamma \in H^2(\Gamma_h)$ and $[\![\ell_\Gamma \boldsymbol{\nu}_\Gamma^\tau \nabla p_\Gamma]\!] = 0$ on $\mathcal{E}_{\Gamma,h}^I$. Moreover, for every $F \in \Gamma_h$, it holds $\mathscr{E}_\Gamma p_\Gamma|_{T_F} \in H^{r_F}(T_F)$, with $r_F \geq 1 + (d-1)/2$ and $T_F \in \mathcal{F}_\#$ with $F \subset T_F$.*

We can now state the main convergence result.

Theorem 4.3. *Let $\mathcal{T}_\# = \{T_E\}$ and $\mathcal{F}_\# = \{T_F\}$ denote the associated coverings of Ω and Γ, respectively, consisting of shape-regular simplexes. Let $(p, \boldsymbol{u}, p_\Gamma)$ be the solution of problem* (2) *and $\big((p_h, \boldsymbol{u}_h), p_{\Gamma,h}\big) \in Q_h^b \times \boldsymbol{W}_h^b \times Q_h^\Gamma$ be its approximation obtained with the method* (3) *with the penalization parameters given by* (4) *and $\sigma_{0,\Gamma}$ sufficiently large. Moreover, suppose that the exact solution $(p, \boldsymbol{u}, p_\Gamma)$ satisfies the regularity Assumption 4.2. Then, the following error bounds hold:*

$$|||(p, p_\Gamma) - (p_h, p_{\Gamma,h})|||^2 \lesssim \sum_{E\in\mathcal{T}_h} \frac{h_E^{2(s_E-1)}}{k_E^{2(r_E-1)}} G_E ||\mathscr{E}p||^2_{H^{r_E}(T_E)} + \sum_{F\in\Gamma_h} \frac{h_F^{2(s_F-1)}}{k_F^{2(r_F-1)}} G_F ||\mathscr{E}_\Gamma p_\Gamma||^2_{H^{r_F}(T_F)},$$

$$||\boldsymbol{u} - \boldsymbol{u}_h||^2_{0,\mathcal{T}_h} \lesssim \sum_{E\in\mathcal{T}_h} \frac{h_E^{2(s_E-1)}}{k_E^{2(r_E-1)}} G_E ||\mathscr{E}p||^2_{H^{r_E}(T_E)} + \sum_{F\in\Gamma_h} \frac{h_F^{2(s_F-1)}}{k_F^{2(r_F-1)}} G_F ||\mathscr{E}_\Gamma p_\Gamma||^2_{H^{r_F}(T_F)},$$

where the $\mathscr{E}p$ is to be interpreted as $\mathscr{E}_1 p_1$ when $E \subset \Omega_1$ or as $\mathscr{E}_2 p_2$ when $E \subset \Omega_2$. Here, $s_E = \min(k_E + 1, r_E)$ and $s_F = \min(k_F + 1, r_F)$ and the constants G_E and G_F are defined

as:

$$G_E = \bar{\boldsymbol{\nu}}_E + h_E k_E^{-1} \max_{F\subset\partial E\setminus\Gamma} \sigma_F + (\alpha_\Gamma + \beta_\Gamma) h_E k_E^{-1} + (1+B)\bar{\boldsymbol{\nu}}_E^2 h_E^{-1} k_E \max_{F\subset\partial E\setminus\Gamma} \sigma_F^{-1} + (1+B)\bar{\boldsymbol{\nu}}_E^2 h_E^{-1} k_E^2 \max_{F\subset\partial E\setminus\Gamma} \sigma_F^{-1},$$

$$G_F = \bar{\boldsymbol{\nu}}_F^\tau \ell_\Gamma + h_F k_F^{-1} \max_{e\subseteq\partial F} \sigma_e + \alpha_\Gamma h_F^2 k_F^{-2} + (\bar{\boldsymbol{\nu}}_F^\tau \ell_\Gamma)^2 h_F^{-1} k_F \max_{e\subseteq\partial F} \sigma_e^{-1} + (\bar{\boldsymbol{\nu}}_F^\tau \ell_\Gamma)^2 h_F^{-1} k_F^2 \max_{e\subseteq\partial F} \sigma_e^{-1}.$$

5 Numerical experiments

We present a two-dimensional numerical experiment, implemented in MATLAB®, with the aim of validating the obtained theoretical convergence results. We employ polygonal Voronoi meshes conforming to the fracture generated with [8]. We take $\Omega = (0,1)^2$ cut by the fracture $\Gamma = \{(x,y)\in\Omega : \ x+y=1\}$, and choose as exact solutions in the bulk and in the fracture

$$p = \begin{cases} e^{x+y} & \text{in } \Omega_1, \\ e^{x+y} + \frac{4\eta_\Gamma}{\sqrt{2}} e & \text{in } \Omega_2, \end{cases} \qquad \mathbf{u} = \begin{cases} -e^{x+y} & \text{in } \Omega_1, \\ -e^{x+y} & \text{in } \Omega_2, \end{cases} \qquad p_\Gamma = e + \frac{2\eta_\Gamma}{\sqrt{2}} e,$$

which satisfy the model problem (2) for $\xi = 1$, $\ell_\Gamma = 0.001$ and $\boldsymbol{\nu} = \boldsymbol{\nu}_\Gamma = \mathbf{I}$. In order to test the h-convergence properties of our method, we split the error in the two contributions given by the bulk and fracture errors. All the plots in Figure 1 show the computed errors as a function of the inverse of the mesh size (loglog scale), together with the expected convergence rates. Each plot consists of four lines: every line shows the behaviour of the computed error for a different polynomial degree in the bulk (we consider $k = 1,2,3,4$). For the fracture problem we always choose $k_\Gamma = 2$. The theoretical convergence rates are clearly achieved. For the fracture error we observe a loss of accuracy for $k = 4$, probably due to the particular test case and round of errors. An extensive numerical study is under investigation and will be the subject of future research.

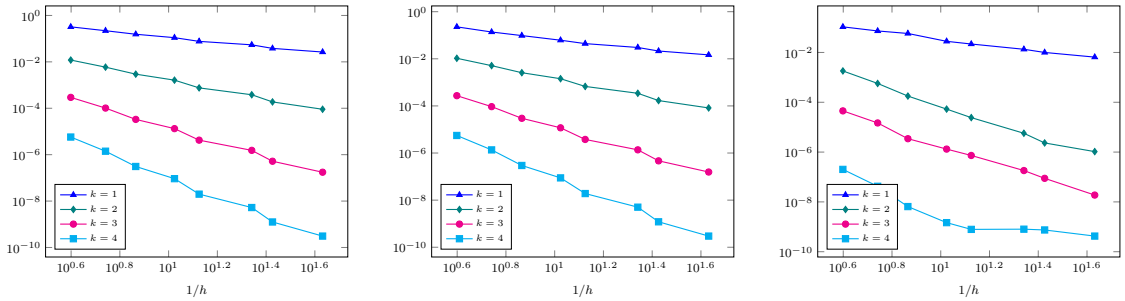

(a) $||p - p_h||_{1,\Omega}$ (b) $||\mathbf{u} - \mathbf{u}_h||_{0,\Omega}$ (c) $||p^\Gamma - p_h^\Gamma||_{1,\Gamma}$

Figure 1: Example 1: Computed errors as a function of $1/h$ (loglog scale) and expected convergence rates for bulk polynomial degree $k = 1,2,3,4$ and fracture polynomial degree $k_\Gamma = 2$.

References

[1] P. F. Antonietti, C. Facciolà, A. Russo, and M. Verani. Discontinuous Galerkin Approximation of Flows in Fractured Porous Media on Polytopic Grids. *SIAM J. Sci. Comput.*, 41(1):A109–A138, 2019.

[2] D. N. Arnold. An interior penalty finite element method with discontinuous elements. *SIAM J. Numer. Anal.*, 19(4):742–760, 1982.

[3] D. N. Arnold, F. Brezzi, B. Cockburn, and L. D. Marini. Unified analysis of discontinuous Galerkin methods for elliptic problems. *SIAM J. Numer. Anal.*, 39(5):1749–1779, 2001/02.

[4] A. Cangiani, Z. Dong, E. H. Georgoulis, and P. Houston. *hp-Version discontinuous Galerkin methods on polygonal and polyhedral meshes*. SpringerBriefs in Mathematics. Springer International Publishing, 2017.

[5] B. Cockburn and C.-W. Shu. The local discontinuous Galerkin method for time-dependent convection-diffusion systems. *SIAM J. Numer. Anal.*, 35(6):2440–2463, 1998.

[6] V. Martin, J. Jaffré, and J. E. Roberts. Modeling fractures and barriers as interfaces for flow in porous media. *SIAM J. Sci. Comput.*, 26(5):1667–1691, 2005.

[7] I. Perugia and D. Schötzau. An *hp*-analysis of the local discontinuous Galerkin method for diffusion problems. *J. Sci. Comput.*, 17(1):561–571, 2002.

[8] C. Talischi, G. H. Paulino, A. Pereira, and I. F. Menezes. Polymesher: a general-purpose mesh generator for polygonal elements written in matlab. *Structural and Multidisciplinary Optimization*, 45(3):309–328, 2012.

[9] M. F. Wheeler. An elliptic collocation-finite element method with interior penalties. *SIAM J. Numer. Anal.*, 15(1):152–161, 1978.

MOX Technical Reports, last issues

Dipartimento di Matematica
Politecnico di Milano, Via Bonardi 9 - 20133 Milano (Italy)

10/2019 Abramowicz, K.; Pini, A.; Schelin, L.; Sjostedt de Luna, S.; Stamm, A.; Vantini, S.
Domain selection and family-wise error rate for functional data: a unified framework

11/2019 Benacchio, T.; Klein, R.
A semi-implicit compressible model for atmospheric flows with seamless access to soundproof and hydrostatic dynamics

12/2019 Capezza, C.; Lepore, A.; Menafoglio, A.; Palumbo, B.; Vantini, S.
Control charts for monitoring ship operating conditions and CO2 emissions based on scalar-on-function regression

13/2019 Manzoni, A; Quarteroni, A.; Salsa, S.
A saddle point approach to an optimal boundary control problem for steady Navier-Stokes equations

09/2019 Antonietti, P.F.; Facciola', C.; Verani, M.
Unified analysis of Discontinuous Galerkin approximations of flows in fractured porous media on polygonal and polyhedral grids

08/2019 Prouse, G.; Stella, S.; Vergara, C.; Engelberger, S.; Trunfio, R.; Canevascini, R.; Quarteroni, A
Computational analysis of turbulent haemodynamics in radiocephalic arteriovenous fistulas with different anastomotic angles

06/2019 Pagani, S.; Manzoni, A.; Carlberg, K.
Statistical closure modeling for reduced-order models of stationary systems by the ROMES method

07/2019 Dal Santo, N.; Manzoni, A.
Hyper-reduced order models for parametrized unsteady Navier-Stokes equations on domains with variable shape

05/2019 Gasperoni, F.; Ieva, F.; Paganoni, A.M.; Jackson, C.; Sharples, L.
Evaluating the effect of healthcare providers on the clinical path of Heart Failure patients through a novel semi-Markov multi-state model

04/2019 Delpopolo Carciopolo, L.; Formaggia, L.; Scotti, A.; Hajibeygi, H.
Conservative multirate multiscale simulation of multiphase flow in heterogeneous porous media